ChemPubSoc Europe

DOI: 10.1002/slct.201601164

Chemistry SELECT Communications

Materials Science inc. Nanomaterials & Polymers

Mesoporous TiO_2 Thin Film Formed From a Bioinspired Supramolecular Assembly

Yi-Chen Wu,[a, b] Y. S. Lu,[a] Bishnu Prasad Bastakoti,[b] Yunqi Li,[b] Malay Pramanik,[b] M. Shahriar Hossain,[c] Ekrem Yanmaz,[d] and Shiao-Wei Kuo*[a]

In this study we synthesize a novel mesoporous titanium oxide (TiO_2) through calcination of a bioinspired supramolecular assembly of polymeric micelles, based on the thymine-functionalized homopolymer, poly(4-vinylbenzyl triazolylmethyl-methylthymine), complexed with $Ti(OH)_2^{2+}$ ions. We characterize thin films of these structures using wide-angle X-ray diffraction, small-angle X-ray scattering, nitrogen adsorption/desorption isotherms, transmission electron microscope, and scanning electron microscope. This approach is simple, effective, and inexpensive when compared with the synthesis of diblock or triblock copolymers typically required to prepare soft templates. This new mesoporous material exhibits superior photocatalytic activity for the degradation of the organic dye methylene blue almost three times higher than that of bulk TiO_2.

Monodisperse colloid particles are attractive materials with applications in photonic crystals,[1] biosensors,[2] nanostamps for soft lithography,[3] microlenses,[4] colloidal lithography,[5–6] and porous membranes,[7] and as seed particles for core/shell and hollow spheres.[8] The self-assembly of block copolymers can be used to form core/shell micelle structures with solvent-insoluble cores and solvent-swollen coronas.[9] Nevertheless, because it can be difficult and time-consuming to synthesize diblock and triblock copolymers, the self-assembly of non-covalently connected micelles (NCCMs) has become a very popular approach for the preparation of polymeric micelles from complementary homopolymer pairs.[9,10] In NCCM systems, the components forming the cores and shells are connected through noncovalent intermolecular interactions (e.g. hydrogen bonds) rather than the covalent bonds found within micelles formed from block copolymers.[9] Jiang et al.[11] discovered NCCMs when pursuing a "block- copolymer free" strategy using pairs of complementary homopolymers, such as carboxyl-terminated polystyrene (PS) oligomers and poly(4-vinylpyridine) (P4VP) polymers that formed "graft-like" copolymers in their common solvent, stabilized through hydrogen bonds between the carboxyl and pyridine units.[10–12] Many other polymers [e.g., lightly sulfonated PS/P4VP, poly(styrene-co-methacrylic acid)/polyvinylpyrrolidone, a hydroxyl-functionalized PS/P4VP, and poly(acrylic acid)/polycaprolactone] can be used to prepare several other types of micelle-like structures stabilized through hydrogen- bonding.

The self-assembly of organic molecules can also be combined with inorganic components possessing various electronic, magnetic, or photonic properties as a powerful approach for the synthesis of various nanostructures.[13] For example, Weng et al. synthesized needle-like TiO_2 nanostructures when using a poly(styrene-*b*-4-vinylpyridine) (PS-*b*-P4VP) diblock copolymer as a template.[14] Indeed, the self-assembly of micelle structures into soft templates possessing insoluble hydrophobic cores surrounded by hydrophilic shells has been used widely to prepare mesoporous materials featuring large surface areas, and controllable pore volumes and pore size distributions.[15] Among these mesoporous materials, titanium dioxide TiO_2 particularly versatile because its high chemical stability, high photocatalytic efficiency, low of cost, and non-toxicity facilitate its wide applicability in photocatalysis, photovoltaics, and gas sensing.[16] Notably, TiO_2 also possesses a relatively wide band gap (3.0 eV for the rutile phase; 3.2 eV for the anatase phase) and a high recombination rate for electron/hole pairs.[17–19] Although the rutile phase has lower band gap, the anatase phase displays a lower recombination of photo-generated carriers and a higher reduction ability.[20] The anatase phase typically exhibits much better photocatalytic activity than the rutile phase of TiO_2.[21] This photocatalytic activity can be used under ultraviolet (UV) irradiation to oxidize organic dyes and other compounds into CO_2 and H_2O.[22–23] To take advantage of these excellent properties, the challenge remains to find ways to incorporate TiO_2 nanoparticles into biomimetic materials. We become interested in the study of such non-covalently connected micelles, and the effect of their micelle structures on their environments in bio-

[a] *Y.-C. Wu, Y. S. Lu, S.-W. Kuo*
Materials and Optoelectronic Science
National Sun Yat-Sen University
Center for Nanoscience and Nanotechnology
Kaohsiung, 804, Taiwan
E-mail: kuosw@faculty.nsysu.edu.tw
Homepage: http://smr.nsysu.edu.tw:10080/
[b] *Y.-C. Wu, B. Prasad Bastakoti, Y. Li, M. Pramanik*
World Premier International (WPI) Research Center for Materials Nanoarchitectonics (MANA)
National Institute for Materials Science (NIMS)
1-1 Namiki, Tsukuba, Ibaraki 305-0044 (Japan)
[c] *M. Shahriar Hossain*
Australian Institute for Innovative Materials (AIIM)
University of Wollongong
Squires Way, North Wollongong, NSW 2500, Australia.
[d] *E. Yanmaz*
Department of Mechatronics, Faculty of Engineering and Architecture
Gelisim University, Istanbul 34315, Turkey.

Supporting information for this article is available on the WWW under http://dx.doi.org/10.1002/slct.201601164

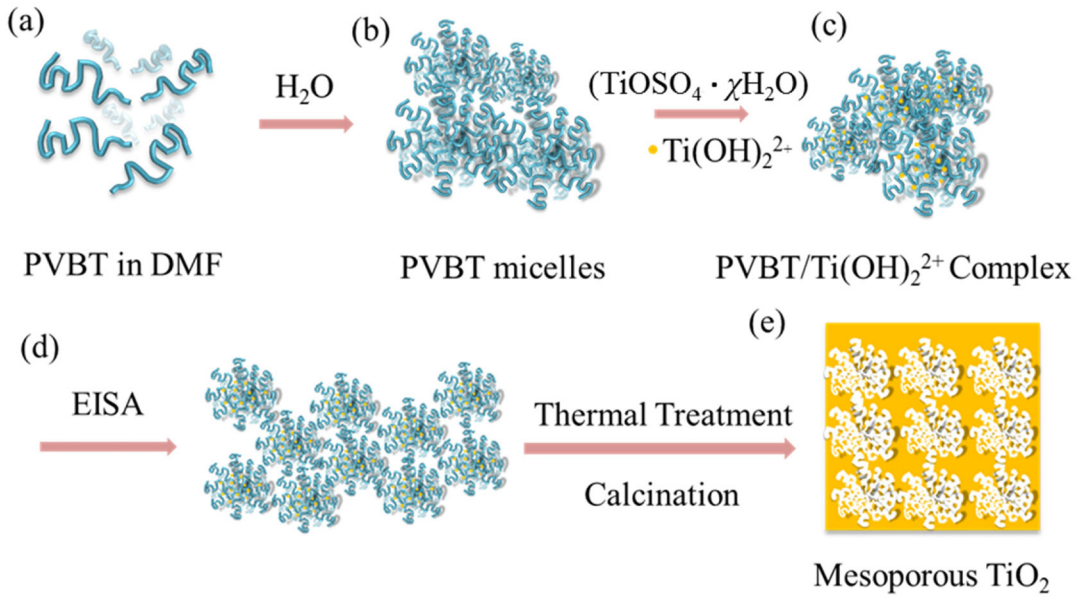

Scheme 1. Schematic representation of the mechanism of formation of a mesoporous TiO_2 film.

logical systems.[24–26] In a previous study, we mimicked DNA-like interactions, namely those between adenine (A) and thymine (T) units, when blending a DNA hetero-nucleobase (T)-containing homopolymer and adenine- terminated poly(ethylene oxide) (PEO–A) homopolymers to form "graft- like" copolymer through complementary multiple hydrogen bond between PEO–A and PVBT.[27–28] Weng[14] and Zhao[29–30] et al. reported that pre-synthesized nanoparticles can be selectively dispersed in one block of a diblock copolymer using specific interactions between their surface ligands and the block. For example, pre-synthesized CdS nanoparticles selectively incorporated into the PS phase of PS-PEO by dipole-dipole interactions.[31–32] In another case, TiO_2 nanostructures have been selectively incorporated into poly(4-vinylpyridine) of the diblock copolymer (PS-*b*-P4VP) via ionic-polar interactions.[14] We suspected that similar specific interactions between $Ti(OH)_2^{2+}$ ions and T- nucleobases might be useful for the preparation of a new material capable of removing pollutants (dyes, heavy metals) from the environment.

In previous studies,[33] we reported that the T-functionalized homopolymer poly(4-vinylbenzyl triazolylmethyl methylthymine) (PVBT) can form stable micelles through multiple hydrogen bonding in DMF solution; a selective solvent, namely water, led to the formation of core/shell-structured micelles. This simple method can also be applied to form micelles for templates to prepare porous materials. Uniform mesoporous thin films of these materials have been prepared most commonly through evaporation-induced self-assembly (EISA) templated by low-molecular-weight surfactants or Pluronic-type triblock copolymers.[29–30] Herein, we prepared mesoporous TiO_2 thin films templated by bioinspired supramolecular polymeric micelles of PVBT. The schematic diagram for the synthesis of mesoporous TiO_2 film is shown in Scheme 1. We characterized mesoporous TiO_2 using different techniques; wide-angle X-ray diffraction (WAXD), small-angle X-ray scattering (SAXS), nitrogen adsorption/desorption isotherms, transmission electron microscope (TEM), and scanning electron microscope (SEM). The calcined mesoporous TiO_2 exhibited enhanced photo-degradation of methylene blue.

Figure S1 presents a dynamic light scattering (DLS) analysis of the PVBT homopolymer in DMF/H_2O. DMF is a good solvent for PVBT, while H_2O is a poor solvent.[33] The micelle solution was prepared through very slow dropwise addition of H_2O to a solution of PVBT in DMF. The hydrodynamic diameter (D_h) of PVBT in the DMF/H_2O solution was approximately 420 nm, suggesting that the individual polymer chains assembled together to form larger micelles. Thus formed micelles are used as templates for the preparation of mesoporous TiO_2 materials. The reaction solution (micelles and $Ti(OH)_2^{2+}$ ions) was stirred for 2 days to ensure that the $Ti(OH)_2^{2+}$ ions completely diffuse into the micelles and attach to the N–H groups of PVBT through ion-dipole interactions. The thin films of micelles composites were prepared by casting directly over a silicon substrate, the film was annealed at 170 °C under vacuum for 24 h to condense the $Ti(OH)_2^{2+}$ ions into TiO_2, as follows:

$$Ti(OH)_2^{2+} + H_2O \longrightarrow Ti(OH)_2 + 2H^+$$
$$Ti(OH)_2 \xrightarrow{L} TiO_2 + H_2O$$

Figure 1 presents FT-IR spectra of pure PVBT, the PVBT/Ti $(OH)^{2+}$ complex, and the mesoporous TiO_2 obtained after removing the PVBT template by calcination at 450 °C for 6 h. The T units of PVBT in the polymeric micelles could interact with Ti $(OH)^{2+}$ ions through ion-dipole interactions, much like DNA base pairs interact with Hg (II) ions, to form T···Hg···T metal-mediated base pairs as shown in Scheme S1.[34–35] The N–H stretching region of the spectrum of PVBT featured a sharp ab-

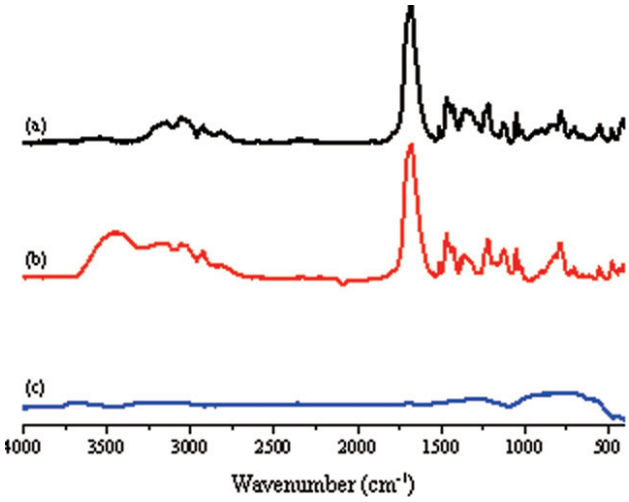

Figure 1. FTIR spectra of (a) pure PVBT, (b) PVBT/$Ti(OH)^{2+}$ complex obtained after heating at 170 °C, and (c) mesoporous TiO_2 obtained after calcination at 450 °C.

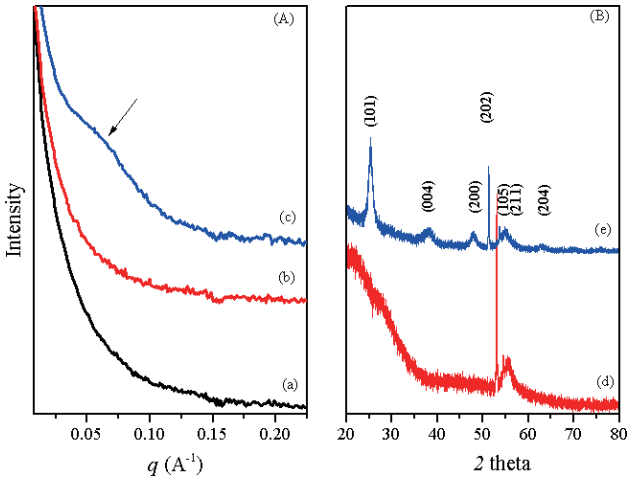

Figure 2. (A) SAXS patterns of (a) pure PVBT, (b) the PVBT/$Ti(OH)^{2+}$ complex obtained after heating at 170 °C, and (c) mesoporous TiO_2 obtained after calcination at 450 °C; (B) WAXD patterns of (d)PVBT/$Ti(OH)^{2+}$ complex obtained after heating at 170 °C, and (e) mesoporous TiO_2 obtained after calcination at 450 °C.

sorption near 3200 cm^{-1} (Figure 1a). This signal shifted to a broad absorption band near 3450 cm^{-1}, for the N–H units of PVBT interacting with $Ti(OH)^{2+}$; in addition, the strong peaks of the free C=O (1716 cm^{-1}) group of the T units of PVBT shifted to relatively lower wavenumbers of 1690 cm^{-1} when PVBT interacted with $Ti(OH)^{2+}$ (Figure 1b).[36] We did not observe any signals from the PVBT polymer after calcination at 450 °C for 6 h (Figure 1c), which ensures the complete removal of the PVBT template.

The calcination process removed the PVBT template and transformed the amorphous TiO_2 framework into a highly crystalline anatase TiO_2 framework. We tested several different calcination temperatures to investigate their effects on the crystallinity and morphology of the final TiO_2 mesoporous structures.[37–38] In general, low-molecular-weight block copolymers (e.g., Pluronic P-123) burnt out at around 250 °C which is much lower than the crystallization temperature of TiO_2 (ca. 350 °C).[39] That's the reason why it is difficult to preserve.

The mesostructure after calcination. In contrast, the PVBT micelles used as template in this study possessed high thermal stability, with a sharp weight loss occurring at approximately 450 °C according to thermogravimetric analysis curve (Figure S2). Moreover, the high residue in the thermogravimetric analysis curve of PVBT suggested that this polymer have thermal stability superior to that of conventional block copolymers (a series of F127 or P123 triblock copolymers).

In spite of using a high calcination temperature to remove the PVBT template, the mesoporous TiO_2 structure was well preserved. We employed SAXS to examine the mesostructure of the TiO_2 product (Figure 2 A). The SAXS patterns of the PVBT micelles used as template and the PVBT/$Ti(OH)^{2+}$ complex did not reveal any evidence for micro-phase separation, with no obvious peaks appearing in Figure 2 A(a) and 2 A(b), respectively. In contrast, we observed evidence for a mesoporous TiO_2 structure after thermal calcination with obvious shoulder peak appearing in Figure 2 A(c). The *d*-spacing of this first short range-order peak was approximately 10 nm. Figure 2(B) presents a WAXD pattern revealing the crystalline phase of the mesoporous TiO_2 obtained after calcination at 450 °C. All of the peaks in the diffraction pattern are fully assignable to the well-crystallized anatase phase of TiO_2, according to the standard (JCPDS card No. 01–075-2544). As the calcination temperature increased, the peak intensity increased. Signals for the formation of the (101), (004), (200), (202), (105), (211), and (204) planes of the TiO_2 anatase phase are clear evident in Figure 2B(e). Figure 3(a-d) display SEM and TEM images revealing

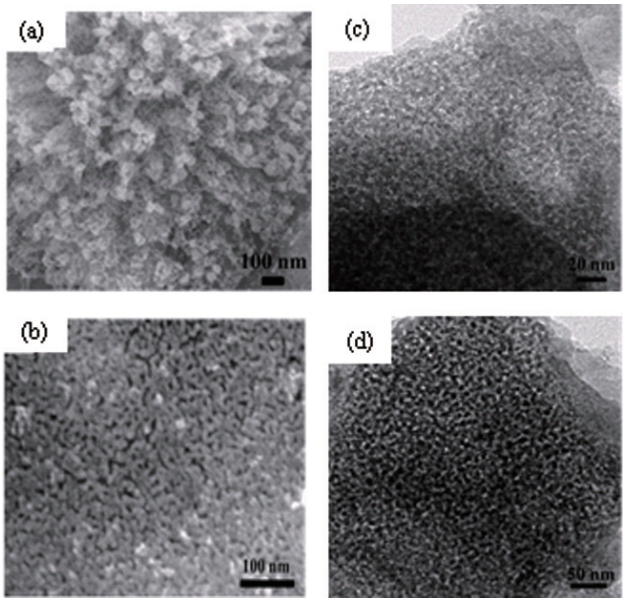

Figure 3. (a-b) SEM images, (c-d) TEM images of mesoporous TiO_2 materials.

the short range-ordered arrangement of the mesoporous TiO_2 structures.

Figure S3(a) presents the corresponding N_2 adsorption/desorption isotherm the typical H_3-like hysteresis loop of a mesoporous structure having slit-like pores. Figure S3(b) reveals that the mean pore sizes, measured from the adsorption branches, were in the range of 5–10 nm, consistent with the SAXS analyses in Figure 2 A. Based on Figure 2 and 3, we conclude that this mesoporous TiO_2 framework possessed a well-crystallized anatase phase.

Figure 3(c) and 3(d) presents high resolution TEM images of the mesoporous structures of TiO_2. The image in Figure 3(c) reveals a porous architecture for the sample, agreement with the SAXD analysis. The pore sizes correspond to the void space formed after combustion of the polymer. The average diameter of 5–10 nm observed in Figure 3(c) is similar to the *d*- spacing of 10 nm found in the SAXS analysis. The selected area electron diffraction pattern [inset to Figure 3(c)] features several diffraction rings corresponding to the TiO_2 (101) and (200) crystal planes. To confirm the formation of mesoporous TiO_2, we also recorded EDX patterns (Figure S4) that revealed Ti signals. The mass percentage of Ti and O are 25.36 % and 74.64 % respectively. We also confirm TiO_2 mesoporosity from EDX mapping images by Figure S5. That indicated Ti and O distributed on the mesoporous. Taken together, these analyses provide clear evidence that the polymeric micelles combined with Ti $(OH)^{2+}$ resulted in the formation of a mesoporous TiO_2 material after calcination. In addition, loss of polymer through calcination left a TiO_2 framework featuring interconnecting spherical micelles.

Mesoporous TiO_2 materials have high photocatalytic activity for the degradation of organic dyes that are common by-products in the textile industry. UV irradiation excites TiO_2 to form positive holes, which further oxidize hydroxide ions or water molecules to generate hydroxyl radicals, very strong oxidants capable of transforming organic compounds into salts, CO_2, and H_2O.[37,39–40] We chose methylene blue (MB) for the model reaction, and used UV-Vis spectroscopy to measure the time-dependent concentration of MB in solution. Figure 4(a) compares the absorptions of MB recorded in the presence of pure TiO_2 (without a porous structure) and the mesoporous TiO_2 structure. The mesoporous TiO_2 material adsorbed a huge amount of MB during the first 20 min period prior to UV irradiation. Subsequent photodegradation for 65 min under irradiation at a wavelength (of 254 nm) revealed that the adsorptive capacity of the mesoporous TiO_2 material was larger than that of non-porous/bulk TiO_2. The mesoporous TiO_2 not only provides sufficient absorption but also enhances stability. In addition, the reaction displayed first-order rate kinetics; we used the MB concentration to evaluate the rates of photocatalysis from the linear relationships between $\ln(C/C_o)$ and time from the equation $\ln(C/C_0) = kt + A$. Here C is the concentration in the solution after irradiation, and C_0 is the initial concentration before irradiation; k represents the reaction rate constant. The calculated values of k in Figure 4(b) reveal that the mesoporous TiO_2 ($k = 3.76 \times 10^{-3}$ min^{-1}) degraded MB faster than did the pure TiO_2 ($k = 1.29 \times 10^{-3}$ min^{-1}); indeed, the photo-

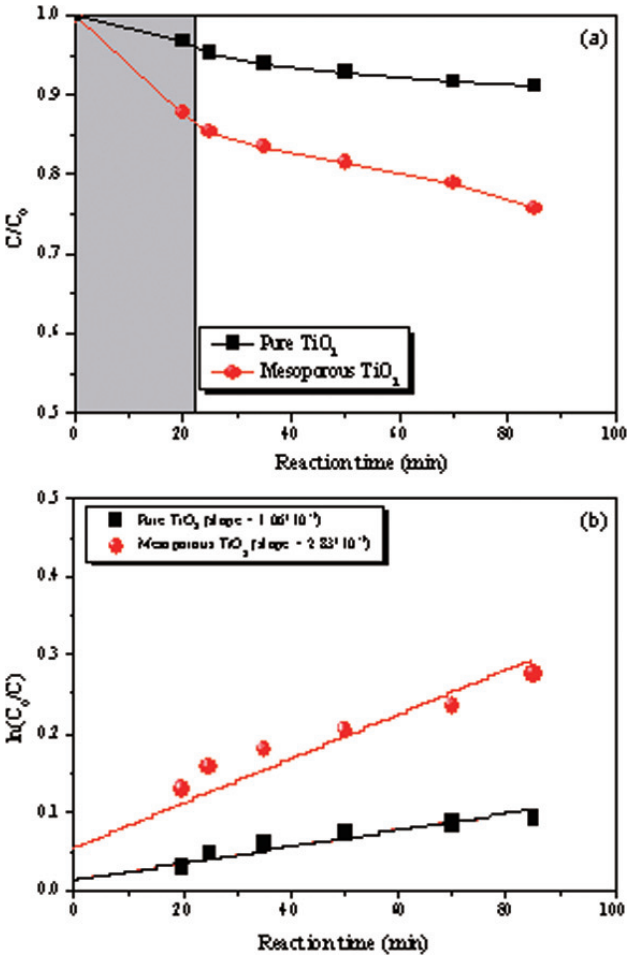

Figure 4. (a) Initial adsorption of MB molecules for 20 min and then photodegradation for 65 min under UV irradiation and (b) Kinetics of MB degradation. A pure TiO_2 and mesoporous TiO_2 film calcined at 450 °C on quartz substrate was dipped into a MB solution (3 ml; 2×10^{-5} M) in dark at room temperature for 20 min. Subsequent put under UV irradiation and keep the same distance (approximately 10 cm) between the UV lamp and the surface of the mixed solution. The concentration of MB in the solution was monitored by UV/Vis spectrometer.

degradation rate of the former was triple that of the latter. Therefore, we anticipate that this new method for the synthesis of mesoporous materials using homopolymer as templates might have substantial impact on environmental remediation.

Conclusions

We have developed a new soft template, thymine -functionalized homopolymer, for the preparation of mesoporous TiO_2 materials. The thymine plays an important role in micellization of homopolymer and provides active sites for inorganic precursors. It also assists the supramolecular assembly process as well as the connection of the spherical micelles to form the TiO_2 mesostructure. The mesoporous TiO_2 showed superior photocatalytic performance than bulk TiO_2. The approach we have used in this study opens up new possibilities for using biomimetic materials as soft templates to prepare mesoporous

materials with different compositions. This concept seems quite simple, effective, and potentially widely applicable to other nucleobase composites.

Supporting Information

Supporting information contains detailed description including the materials of experimental; materials synthesized steps, total experimental steps, characterization, and the detailed other experimental data of mesoporous TiO_2.

Acknowledgements

This study was financially supported by the Ministry of Science and Technology, Taiwan, under contracts MOST 103–2221-E-110-079-MY3. Dr. Yi-Chen Wu also would like to thank 2014 New Partnership Program for the Connection to the Top Labs in the World, also supported by the Ministry of Science and Technology, Taiwan, under contracts MOST 103–2911-I-110-513 that helped initiate this study.

Keywords: TiO_2 · Supramolecular Assembly · Bioinspired Materials

[1] G. R. Yi, J. H. Moon, V. N. Manoharan, D. J. Pine, S. M. Yang, *J. Am. Chem. Soc.* **2002**, *124*, 13354–13355.
[2] A. J. Haes, W. P. Hall, L. Chang, W. L. Klein, R. P. Van Duyne, *Nano Lett.* **2004**, *4*, 1029–1034.
[3] X. Chen, Z. Chen, N. Fu, G. Lu, B. Yang, *Adv. Mater.* **2003**, *15*, 1413–1417.
[4] M. H. Wu, G. M. Whitesides, *Appl. Phys. Lett.* **2001**, *78*, 2273–2275.
[5] C. L. Haynes, R. P. Van Duyne, *J. Phys. Chem. B* **2001**, *105*, 5599–5611.
[6] F. Yan, W. A. Goedel, *Adv. Mate.* **2004**, *16*, 911–915.
[7] M. G. Han, S. H. Foulger, *Adv. Mater.* **2004**, *16*, 231–234.
[8] Y. Yu, A. Eisenberg, *J. Am. Chem. Soc.* **1997**, *119*, 8383–8384.
[9] M. Guo, M. Jiang, *Soft Matter* **2009**, *5*, 495–500.
[10] A. O. Moughton, R. K. O'Reilly, *J. Am. Chem. Soc.* **2008**, *130*, 8714–8725.
[11] S. Y. Liu, G. Z. Zhang, M. Jiang, *Polymer* **1999**, *40*, 5449–5453.
[12] S. Y. Liu, Q. M. Pan, J. W. Xie, M. Jiang, *Polymer* **2000**, *41*, 6919–6929.
[13] L. Song, Y. M. Lam, C. Boothroyd, P. W. Teo, *Nanotechnology* **2007**, *18*, 135605–135605-6.
[14] C. C. Weng, K. F. Hsu, K. H. Wei, *Chem. Mater.* **2004**, *16*, 4080–4086.
[15] M. Vallet-Regi. , I. Izquierdo-Barba, M. Colilla, *Phil. Trans. R. Soc. A* **2012**, *370*, 1400–1421.
[16] K. Fujishima, A. Honda, *Nature* **1972**, *238*, 37–38.
[17] T. Froschl, U. Hormann, P. Kubiak, G. Kucerova, M. Pfanzelt, C. K. Weiss, R. J. Behm, N. Husing, U. Kaiser, K. Landfester, M. Wohlfahrt-Mehrens, *Chem. Soc. Rev.* **2012**, *41*, 5313–5360.
[18] M. Batzill, *Energy Environ. Sci.* **2011**, *4*, 3275–3286.
[19] Y. Cong, J. Zhang, F. Chen, M. Anpo, *J. Phys. Chem. C* **2007**, *111*, 6976–6982.
[20] J. B. Joo, Q. Zhang, M. Dahl, I. Lee, J. Goebl, F. Zaera, Y. Yin, *Energy Environ. Sci.* **2012**, *5*, 6321–6327.
[21] G. Liu, J. C. Yu, G. Q. Lu, H. M. Cheng, *Chem. Commun.* **2011**, *47*, 6763–6783.
[22] Q. Xiang, J. Yu, M. Jaroniec, *Chem. Commun.* **2011**, *47*, 4532–4534.
[23] T. Yu, Y. H. Deng, L. Wang, R. L. Liu, L.J. Zhang, B. Tu, D. Y. Zhao, *Adv. Mater.* **2007**, *19*, 2301–2306.
[24] S. Sivakava, J. Wu, C. J. Campo, P. J. Mather, S. J. Rowan, *Chem. Eur. J.* **2006**, *12*, 446–456.
[25] G. M. L. V. Gemert, J. W. Peeters, S. H. M. Sontjens, H. M. Janssen, A. W. Bosman, *Macromol. Chem. Phys.* **2012**, *213*, 234–242.
[26] M. Jiang, M. Li, M. Xiang, H. Zhou, *Adv. Polym. Sci.* **1999**, *146*, 121–196.
[27] Y. C. Wu, S. W. Kuo, *Polym. Chem.* **2012**, *3*, 3100–3111.
[28] Y. C. Wu, Y. S. Wu, S. W. Kuo, *Macromol. Chem. Phys.* **2013**, *214*, 563–571.
[29] D. Y. Zhao, J. L. Feng, Q. S. Huo, N. Melosh, G. H. Fredrickson, B. F. Chmelka, G. D. Stucky, *Science* **1998**, *279*, 548–552.
[30] D. Y. Zhao, Q. S. Huo, J. L. Feng, B. F. Chmelka, G. D. Stucky, *J. Am. Chem. Soc.* **1998**, *120*, 6024–6036.
[31] S. W. Yeh, K. H. Wei, Y. S. Sun, U. S. Liang, K. S. Liang, *Macromolecules* **2003**, *36*, 7903–7909.
[32] U. S. Jeng, Y. S. Sun, H. Y. Lee, C. H. Hsu, K. S. Liang, S. W. Yeh, K. H. Wei, *Macromolecules* **2004**, *37*, 4617–4622.
[33] Y. S. Wu, Y. C. Wu, S. W. Kuo, *Polymers* **2014**, *6*, 1827–1845.
[34] Y. Miyake, H. Togashi, M. Tashiro, H. Yamaguchi, S. Oda, M. Kudo, Y. Tanaka, Y. Kondo, R. Sawa, T. Fujimoto, T. Machinami, A. Ono, *J. Am. Chem. Soc.* **2006**, *128*, 2172–2173.
[35] T. Uchiyama, T. Miura, H. Takeuchi, T. Dairaku, T. Komuro, T. Kawamura, Y. Kondo, L. Benda, V. Sychrovsky, P. Bour, I. Okamoto, A. Ono, *Nucleic Acid Res.* **2012**, 1–9.
[36] C. W. Huang, M. H. Mohamed, C. Y. Zhu, S. W. Kuo, *Macromolecules* **2016**, *49*, 5374–5385.
[37] Y. Li, B. P. Bastakoti, M. Imura, S. M. Hwang, Z. Sun, J. H. Kim, S. X. Dou, Y. Yamauchi, *Chem. Eur. J.* **2014**, *20*, 6027–6032.
[38] B. P. Bastakoti, N. L. Torad, Y. Yamauchi, *ACS Appl. Mater. Interfaces* **2014**, *6*, 854–860.
[39] M. B. Zakaria, N. Suzuki, N. L. Torad, M. Matsuura, K. Maekawa, H. Tanabe, Y. Yamauchi, *Eur. J. Inorg. Chem.* **2013**, *13*, 2330–2335.
[40] N. Suzuki, X. F. Jiang, L. Radhakrishnan, K. Takai, K. Shimasaki, Y. T. Huang, N. Miyamoto, Y. Yamauchi, *Bull Chem. Soc. Jpn.* **2011**, *84*, 812–817.

Submitted: August 23, 2016
Accepted: August 26, 2016